

Orbital and Bonding Anisotropy in a Half-Filled GaFeO₃ Magnetolectric Ferrimagnet

J.-Y. Kim,¹ T. Y. Koo,¹ and J.-H. Park^{1,2,*}

¹*Pohang Accelerator Laboratory, Pohang University of Science and Technology, Pohang, Korea*

²*Department of Physics & electron Spin Science Center, Pohang University of Science and Technology, Pohang, Korea*

(Received 5 September 2005; published 30 January 2006)

We investigated the orbital anisotropy of GaFeO₃ using the Fe *L*_{2,3}-edge x-ray magnetic circular dichroism and the polarization dependent O *K*-edge x-ray absorption spectroscopy. We found that the system shows a considerably large orbital momentum and anisotropic Fe-O bonding, which are unexpected in a half-filled *d*⁵ system such as GaFeO₃. The orbital and bonding anisotropies, which turn out to be induced by the lattice distortions with exotic off-centering site movements, contribute the large magnetocrystalline energy and magnetoelasticity. These results provide critical clues on the microscopic understanding of the magnetolectricity.

DOI: [10.1103/PhysRevLett.96.047205](https://doi.org/10.1103/PhysRevLett.96.047205)

PACS numbers: 75.80.+q, 75.30.Gw, 75.50.Gg, 78.70.Dm

Recently, multiferroic materials, in which magnetism and ferroelectricity coexist, have taken so much attention due to the potential technological applications using the so called magnetolectric (ME) effect. It means that one can change magnetic polarization through an applied electric field or electric polarization through an applied magnetic field. Since the early reports of the multiferroic ME effect on GaFeO₃ and Ni₃B₇O₁₃I [1,2], the ME effect has been reported for various multiferroic materials [3–6]. In spite of its interesting characteristics, the ME effect has been mostly discussed in a limit of conceptual macroscopic pictures like nonlinear second-order susceptibilities, i.e., response of electric or magnetic polarization to an applied magnetic or electric field, respectively.

Some microscopic approaches have been suggested based on band structure calculations or model Hamiltonians selectively for manganites with a *d*⁴ configuration [7–9]. The system contains strong anisotropy in bonds between neighboring ions, which are induced by orbital ordering or orbital anisotropy. An applied magnetic field makes the ordered spins tilt and reduces the magnetic coupling energy, $JS_i \cdot S_j$. Then the lattice becomes distorted to compensate the coupling energy and induces electric polarization, the so called magnetoelasticity. Indeed, the multiferroicity has been founded mostly in the manganites such as YMnO₃, BiMnO₃, TbMnO₃, TbMn₂O₅, etc. [3–6]. The situation, however, is rather different in GaFeO₃, in which ferrimagnetism and piezoelectricity coexist. The ionic state is Fe³⁺ with a half-filled 3*d*⁵ configuration, in which the orbital momentum $L = 0$ and even lattice distortions can not contribute any orbital anisotropy. Thus the magnetolectric effect has been puzzled over and discussed only conceptually although various optical and x-ray magnetolectric phenomena have been demonstrated in this system [10–12].

In this Letter, we report abnormal orbital anisotropy in a half-filled *d*⁵ system GaFeO₃, which is induced by the anisotropic Fe-O bond. The x-ray magnetic circular dichroism (XMCD) at Fe *L*_{2,3} edges shows a considerably large

orbital momentum. The O *K*-edge x-ray absorption spectroscopy (XAS) shows strong polarization dependence, especially in the region of the Fe 3*d* states. In spite of the half-filled ionic state with $L = 0$, the system has a nonvanishing *L* value due to the anisotropic O 2*p* to Fe 3*d* charge transfer, which results from the anisotropic hybridization. These results demonstrate that crystalline distortions contribute the orbital momentum through the anisotropic Fe 3*d*–O 2*p* hybridization and the large magnetocrystalline anisotropy, and suggest that the magnetolectric effect in GaFeO₃ can be understood in the framework of the large magnetoelasticity originated from the strong anisotropic bonding as in the multiferroic manganites. However, different from the manganites, GaFeO₃ contains the bond anisotropy induced by the lattice distortions due to exotic off-centering ionic movements, not by the Jahn-Teller type orbital anisotropy due to the partially filled orbital state.

Untwined high quality GaFeO₃ single crystals were grown by a flux method. The XAS and XMCD measurements were carried out at the Pohang Light Source (PLS) elliptically polarized undulator beam line 2A1. The samples were oriented along the crystal axes for the measurements and introduced into an experimental chamber with the base pressure of 5×10^{-10} Torr. The O *K*-edge XAS spectra were simultaneously collected in the total electron yield (TEY) mode and the fluorescence yield mode, which have probing depths of 50 to 100 Å and more than 1000 Å, respectively. The spectra in the two different modes turned out to be nearly identical, indicating that the system is so stable that surface contamination effects are negligible even in the TEY spectra. The crystal structure is orthorhombic with four different cation sublattices, one tetrahedral (*T_d*) Ga1, and three octahedral (*O_h*) Ga2, Fe1, and Fe2 sublattices, as shown in Fig. 1(a). Since the ionic sizes of Ga and Fe are similar to each other, Fe and Ga can be distributed in the four sublattices although Fe (Ga) ions are expected to occupy mainly Fe1 (Ga1) and Fe2 (Ga2) sublattices [13–16]. The

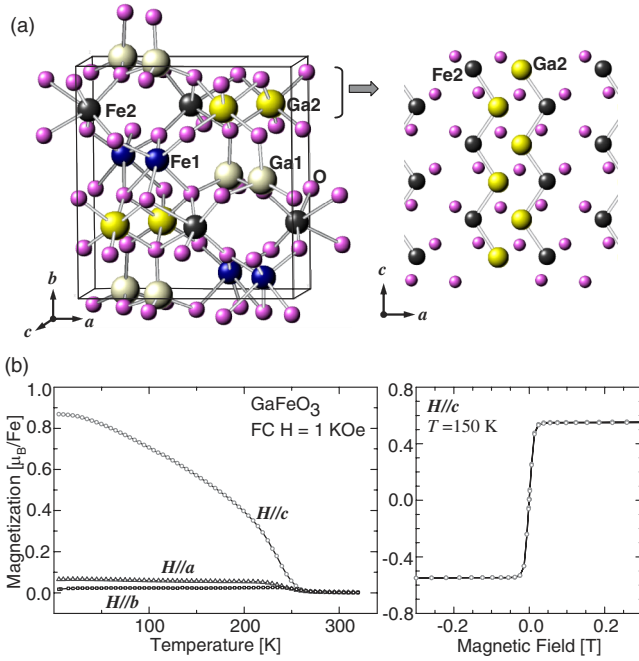


FIG. 1 (color online). (a) Crystal structure of GaFeO₃. Ga1, Ga2, Fe1, and Fe2 sublattices and O atoms are presented in different shades (colors online). The right panel shows the Ga2 and Fe2 sublattice layer structure. (b) Magnetization curves as functions of temperature (M vs T) and an applied magnetic field (M vs H).

magnetization curves as functions of temperature (M vs T) and an applied magnetic field (M vs H), which were measured by using the superconducting quantum interference device (SQUID), are presented in Fig. 1(b). We obtained the net ordered moment $\mu = 0.87\mu_B/\text{Fe}$ at 4 K and the Curie temperature $T_C \approx 260$ K [16]. The system also shows strong magnetic anisotropy with the easy axis along the c axis and the hardest axis along the b axis, indicating a considerably large magnetocrystalline energy, which is attributed to the spin-orbit coupling.

In order to investigate the origin of the magnetocrystalline energy, we performed the XMCD measurements at Fe $L_{2,3}$ edges, which enable us to estimate the spin and orbital momentum separately [17–19]. The energy resolution was 0.3 eV, and the spectra were measured in the TEY mode. A 0.1 T electromagnet was used to switch the magnetization direction in the c axis. The sample temperature was kept at 190 K, where the charging effect due to the insulating character of the sample is not observable in the measurements [20]. The magnetization direction is flipped to be parallel (ρ_+) and antiparallel (ρ_-) to the photon helicity vector at each data point. Figure 2(a) shows the absorption spectra for the different magnetization directions (ρ_+ and ρ_-), and the dichroism ($\Delta\rho$) and its integration. The degree of the circular polarization (95%) of the incident light was taken into account in the spectra. The spectra (ρ_+ and ρ_-), which result from the Fe $2p \rightarrow 3d$ dipole tran-

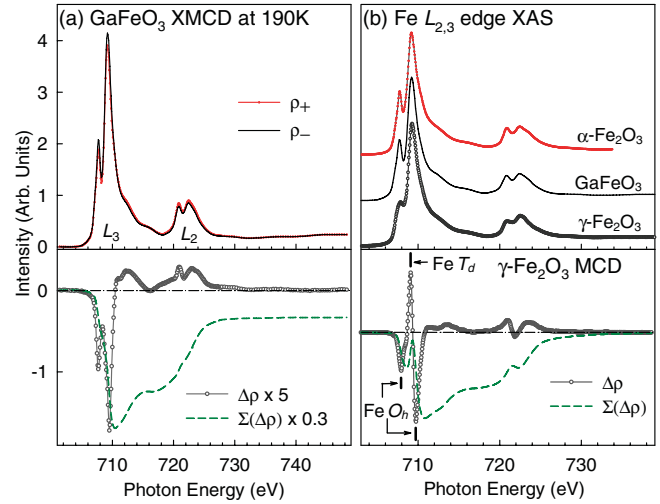


FIG. 2 (color online). (a) Fe $L_{2,3}$ -edge XMCD spectra (ρ_+ and ρ_-), MCD signal, $\Delta\rho$, and its integration, $\Sigma(\Delta\rho)$, of GaFeO₃. (b) XAS spectrum of GaFeO₃ at 190 K in comparison with those of reference iron oxides, α -Fe₂O₃ and γ -Fe₂O₃. The MCD spectrum and its integration of γ -Fe₂O₃ at 80 K are shown at the bottom for comparison.

sition, are divided roughly into the L_3 ($2p_{3/2}$) and L_2 ($2p_{1/2}$) regions. According to the spin sum rule, the spin magnetic moment M_S is estimated to be $0.37 \pm 0.05\mu_B/\text{Fe}$ [21]. Interestingly, the integration of the dichroism ($\Delta\rho$) over the entire $L_{2,3}$ absorption region, which is proportional to the orbital magnetic moment, M_O , is quite considerable. M_O is estimated to be $0.017 \pm 0.002\mu_B/\text{Fe}$ parallel to M_S , and yields the total moment of $0.39 \pm 0.05\mu_B/\text{Fe}$, which is consistent with the SQUID value of $0.43\mu_B/\text{Fe}$ at 190 K. The absolute M_O is small since the measurements were performed at 190 K and the system is a ferrimagnet. But it gives $M_O/M_S = 0.046$, which corresponds to $L = 0.23 \pm 0.04$ for each Fe³⁺ ion under an assumption of $S = 5/2$ [22]. This value is unexpectedly large for the half-filled d^5 system. In γ -Fe₂O₃, which is also a ferrimagnet with Fe³⁺ ions, the XMCD shows that $M_O/M_S \approx 0$ and $L \approx 0$.

Additionally, the XAS and XMCD results provide information on the Fe occupations out of the four different sublattices. Figure 2(b) shows the XAS spectrum of GaFeO₃ in comparison with those of reference Fe-oxides, α -Fe₂O₃ with only O_h Fe³⁺ sites and γ -Fe₂O₃ with a mixture of T_d and O_h Fe³⁺ sites [23]. The spectral line shape of GaFeO₃ is nearly identical to that of α -Fe₂O₃ but somewhat different from that of γ -Fe₂O₃ in both L_3 and L_2 regions. Further, the MCD spectrum of γ -Fe₂O₃, which displays the sum of the contributions from the T_d and O_h sites, is completely different from that of GaFeO₃ with only the contribution from the O_h sites. From these results, one can confidentially conclude that the Fe occupation at the Ga1 T_d site in GaFeO₃ is negligible [16]. This is consistent with Gilleo's simple model proposed early on

[24]. In the model, the fraction of the Fe ion occupation was suggested to be 0, 0.35, 0.825, and 0.825 at the Ga1, Ga2, Fe1, and Fe2 sites, respectively. The Fe^{3+} ($S = 5/2$) spins at the Fe1 sites are antiparallel to those at the Fe2 and Ga2 sites [13], and thus the net moment becomes $0.86\mu_B/\text{Fe}$, which coincides with the obtained moment $0.87\mu_B/\text{Fe}$.

It is quite curious what is the origin of the unexpected orbital momentum in this half-filled system. The polarization dependent O K -edge XAS is one appropriate probe for the investigation since it directly provides the orbital selective unoccupied electronic structure through the hybridization with O $2p$ states. The incident light was set to have $\sim 98\%$ linear polarization. The elliptically polarized undulator enables us to switch the polarization \mathbf{E} vector of the normal incident light 90° without any change of the experimental geometry. The spectra were measured in the $\mathbf{E} \parallel \mathbf{c}$ and $\mathbf{E} \parallel \mathbf{a}$ polarizations and in the $\mathbf{E} \parallel \mathbf{c}$ and $\mathbf{E} \parallel \mathbf{b}$ polarizations by exposing the front and the side of a bar shaped crystal, respectively. The $\mathbf{E} \parallel \mathbf{c}$ spectrum was con-

firmed to be identical for the two measurement geometries. Figure 3(a) shows the XAS spectra measured at 300 K in the TEY mode for three different polarizations, $\mathbf{E} \parallel \mathbf{a}$, $\mathbf{E} \parallel \mathbf{b}$, and $\mathbf{E} \parallel \mathbf{c}$. The photon energy resolution was ~ 0.15 eV. As shown in the inset, the spectra consist of states induced by Fe $3d$ and Ga $3s, p$ /Fe $4s, p$ at low and high photon energies, respectively. Here we will focus on the Fe $3d$ region, which is correlated with the orbital magnetic moment and the ME effect. This region is again divided into the low lying t_{2g} and high lying e_g orbital bands with the energy separation $10Dq \sim 1.4$ eV. The spectra display large spectral variation depending on the polarization vector \mathbf{E} , and show that both the t_{2g} and e_g states are split into two states with energy splitting of ~ 0.04 eV and ~ 0.4 eV, respectively, as depicted schematically in Fig. 3(b). The spectral variations and the orbital states can be understood by the polarization dependent selectivity and the crystal distortions.

The local FeO_6 octahedra at the Ga2, Fe1, and Fe2 sites are distorted trigonally as shown in the view from the b axis in Fig. 3(c). Under the D_{3d} trigonal symmetry, the triplet t_{2g} orbital is split into a singlet a_{1g} orbital along the b axis and doublet e_g^π orbitals in the ac plane [25]. Further, the system contains zigzag chains in the ac plane [see Fig. 1(a)], and thus one can expect formation of the a_{1g} band out of the plane and the e_g^π bands in the plane. Thus the a_{1g} band and e_g^π bands are mainly selected by the $\mathbf{E} \parallel \mathbf{b}$ and the $\mathbf{E} \parallel \mathbf{a}, \mathbf{c}$ polarizations, respectively. Under the D_{3d} symmetry, the e_g state, which is denoted the e_g^σ state, keeps the degeneracy. Because of the zigzag chain structure in the ac plane, the e_g^σ orbitals tend to form out-of-plane bands and along the chain bands. But the e_g^σ orbitals are generally towards the ligand oxygen ions, which are not along the crystal axes, and certain intermixing between the bands is inevitable. Therefore, the $\mathbf{E} \parallel \mathbf{b}$ and $\mathbf{E} \parallel \mathbf{c}$ polarizations mainly enhance the out-of-plane (b -direction) and along the chain (c -direction) e_g^σ bands, respectively, while the $\mathbf{E} \parallel \mathbf{a}$ shows the mixed feature.

The energy splitting of the e_g^σ orbitals, which does not occur under the D_{3d} symmetry, is probably due to additional distortions. Indeed, the local structure shows off-centering movements of the Ga2, Fe1, and Fe2 sites in the piezoelectric ab plane as can be seen in the view from the c axis in Fig. 3(c) while the movement of the Ga1 site is negligible. The movement is small for the Ga2 site, but is quite large, even larger than 0.1 \AA , for the Fe1 and Fe2 sites. The Ga2 and Fe2 sites move along the a and b axis, and the Fe1 sites mostly move along the b axis; i.e., the average movement of the three cation sites is along the a and b axis with the larger movement along the b axis. These movements seem to enhance the Fe $3d$ -O $2p$ hybridization strength along the b axis, and push up the corresponding e_g^σ band energetically. The energy splitting as large as ~ 0.4 eV indicates large anisotropy of the

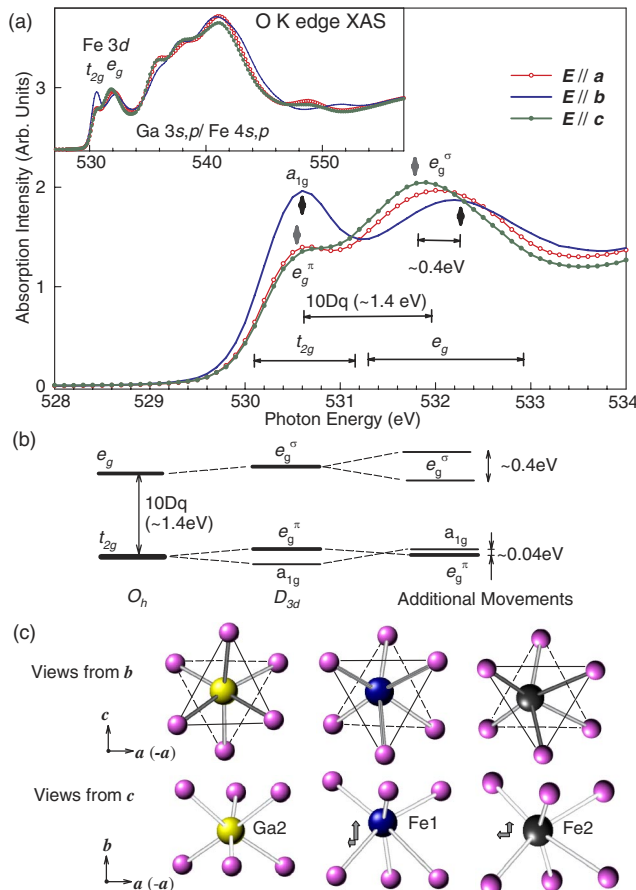


FIG. 3 (color online). (a) Polarization dependent O K -edge XAS spectra at 300 K. The wide range spectra are shown in the inset. (b) Schematic energy diagrams of the crystal field splitting. (b) The local octahedron structures of the Ga2, Fe1, and Fe2 sublattices viewed from the b (upper) and c axis (lower). Thick arrows indicate the off-centering atomic movements.

hybridization strength [26]. The larger hybridization strength along the b axis is also consistent with the relatively large absorption intensity of the a_{1g} band in the t_{2g} region since the absorption intensity reflects the amount of the mixed O $2p$. The larger hybridization is probably the reason why the low lying a_{1g} state under the D_{3d} symmetry is pushed above the e_g^π bands energetically.

Now let us consider the origin of the considerably large orbital magnetic moment and magnetocrystalline energy. The orbital momentum should vanish in the d^5 half-filled Fe^{3+} ions even under crystal distortions, and the isotropic ionic orbital states generally lead to isotropic bonding with oxygen ions as seen in $\gamma\text{-Fe}_2\text{O}_3$. However, in GaFeO_3 , Fe ions move off from the center. These movements induce the large anisotropy in the Fe $3d$ -O $2p$ hybridization and the O $2p$ to Fe $3d$ charge transfer. The orbital momentum can be created by the transferred $3d$ states. The $3d$ atomic orbital momentum is generally quenched by either the O_h or D_{3d} crystal field. It means that the orbitals keep the parity symmetry. As an Fe ion shifts along a certain direction from the center, the parity symmetry of the orbitals becomes broken for axes orthogonal to the direction. Thus, the shift along the b axis (a axis) creates orbital momentums along the c and a axis (c and b axis). Therefore, the shifts of Fe ions along the b and a axis are expected to create the orbital momentum large along the c axis but relatively small along the a and b axis. Further, the hybridization becomes the largest along the b axis and the smallest along the c axis. Thus the hybridized Fe $3d$ orbitals contribute a much larger orbital momentum along the c axis than the a or b axis. Therefore, the magnetic easy axis becomes the c axis due to the microscopic magnetocrystalline energy, which corresponds to the spin-orbit coupling anisotropy energy, $E_{\text{mc}} = -\xi\Delta\mathbf{L} \cdot \mathbf{S}$. The O K -edge XAS and the Fe ionic shifts also suggest that the orbital momentum becomes smaller along the b axis than along the a axis and that the b axis magnetically becomes the hardest. Such magnetic anisotropy completely agrees with the observed magnetization behaviors (M vs T curves) presented in Fig. 1(b).

In summary, we have investigated electronic and orbital anisotropy of multiferroic GaFeO_3 using the Fe $L_{2,3}$ -edge XMCD and the O K -edge XAS. We found that the system has a considerably large orbital momentum and anisotropic Fe-O bonding, which are unexpected in half-filled d^5 systems. The lattice distortions with the off-centering movements of Fe^{3+} octahedron sites in the piezoelectric plane induce the large orbital momentum and orbital anisotropy though the anisotropic Fe $3d$ -O $2p$ hybridization. These results provide a microscopic understanding for the spin-

orbit related phenomena like high anisotropic magnetocrystalline energy and magnetoelasticity.

This work was supported by KOSEF through eSSC at POSTECH, ITEP through the soft x-ray Nano-characterization Program, and the BK21 program.

*Electronic address: jhp@postech.ac.kr

- [1] G. T. Rado, Phys. Rev. Lett. **13**, 335 (1964).
- [2] E. Ascher, H. Rieder, H. Schmid, and H. Stössel, J. Appl. Phys. **37**, 1404 (1966).
- [3] Z. J. Huang, Y. Cao, Y. Y. Sun, Y. Y. Xue, and C. W. Chu, Phys. Rev. B **56**, 2623 (1997).
- [4] A. Moreira dos Santos *et al.*, Solid State Commun. **122**, 49 (2002); T. Kimura *et al.*, Phys. Rev. B **67**, 180401(R) (2003).
- [5] T. Kimura *et al.*, Nature (London) **426**, 55 (2003).
- [6] N. Hur *et al.*, Nature (London) **429**, 392 (2004).
- [7] N. A. Hill, J. Phys. Chem. B **104**, 6694 (2000).
- [8] B. B. van Aken, T. T. M. Palstra, A. Filippetti, and N. A. Spaldin, Nat. Mater. **3**, 164 (2004).
- [9] D. V. Efremov, J. van der Brink, and D. I. Khomskii, Nat. Mater. **3**, 853 (2004).
- [10] Y. Ogawa *et al.*, Phys. Rev. Lett. **92**, 047401 (2004).
- [11] M. Kubota *et al.*, Phys. Rev. Lett. **92**, 137401 (2004).
- [12] J. H. Jung *et al.*, Phys. Rev. Lett. **93**, 037403 (2004).
- [13] E. F. Bertaut *et al.*, J. Mosc. Phys. Soc. **27**, 433 (1966).
- [14] R. B. Frankel, N. A. Blum, S. Foner, A. J. Freeman, and M. Schieber, Phys. Rev. Lett. **15**, 958 (1965).
- [15] B. F. Levine, C. H. Nowlin, and R. V. Jones, Phys. Rev. **174**, 571 (1968).
- [16] T. Arima *et al.*, Phys. Rev. B **70**, 064426 (2004).
- [17] C. T. Chen *et al.*, Phys. Rev. Lett. **75**, 152 (1995).
- [18] B. T. Thole, P. Carra, F. Sette, and G. van der Laan, Phys. Rev. Lett. **68**, 1943 (1992).
- [19] Y. Teramura, A. Tanaka, and T. Jo, J. Phys. Soc. Jpn. **65**, 1053 (1996).
- [20] We found that the charging problem becomes negligible above 170 K.
- [21] The spin sum rule is known to underestimate M_S by $\sim 10\%$ in Fe ionic systems (Ref. [17]).
- [22] As the charge transfer is considered, L can be reduced by several percentage points.
- [23] $\gamma\text{-Fe}_2\text{O}_3$ is often presented by $\text{Fe}^T\text{Fe}_{5/3}^O\text{O}_4$. Here the spin moments of tetragonal, T , sites are antiparallel to those of the octahedral, O , sites.
- [24] M. A. Gilleo, J. Phys. Chem. Solids **13**, 33 (1960).
- [25] S. Sugano, Y. Tanabe, and H. Kamimura, *Multiplets of Transition-Metal Ions in Crystals* (Academic Press, New York, 1970).
- [26] A difference of about 40% in the hybridization strength was estimated in a simple cluster model.